NASA TECHNICAL NOTE

NASA TN D-5210

VAPOR INGESTION PHENOMENON IN WEIGHTLESSNESS

by Kaleel L. Abdalla and Steven G. Berenyi

Lewis Research Center
Cleveland, Ohio

NATIONAL AERONAUTICS AND SPACE ADMINISTRATION • WASHINGTON, D. C. • MAY 1969

VAPOR INGESTION PHENOMENON IN WEIGHTLESSNESS

By Kaleel L. Abdalla and Steven G. Berenyi

Lewis Research Center
Cleveland, Ohio

NATIONAL AERONAUTICS AND SPACE ADMINISTRATION

For sale by the Clearinghouse for Federal Scientific and Technical Information
Springfield, Virginia 22151 – CFSTI price $3.00

ABSTRACT

An experimental program was conducted in the Lewis Research Center's 2.2-Second Zero-Gravity Facility in which the vapor ingestion phenomenon during draining from flat-bottom, cylindrical tanks was studied in both weightlessness and normal gravity. The vapor ingestion phenomenon in weightlessness was correlated with the Weber number using the critical liquid height prior to vapor ingestion as the significant dimension. The normal-gravity data agreed with a theoretical analysis predicting a Froude number correlation. Liquid residuals were generally higher in weightlessness than in normal gravity. Effects of initial liquid height and liquid properties on the vapor ingestion phenomenon and comparisons of vapor ingestion heights for both environments are also presented.

VAPOR INGESTION PHENOMENON IN WEIGHTLESSNESS

by Kaleel L. Abdalla and Steven G. Berenyi

Lewis Research Center

SUMMARY

An experimental program was conducted in the 2.2-Second Zero-Gravity Facility in which the vapor ingestion phenomenon during draining from flat-bottom, cylindrical tanks was studied in both weightlessness and normal gravity. The vapor ingestion phenomenon in weightlessness was correlated with the Weber number using the critical liquid height prior to vapor ingestion as the significant dimension. The normal-gravity data agreed with a theoretical analysis predicting a Froude number correlation. Liquid residuals were generally higher in weightlessness than in normal gravity. Effects of initial liquid height and liquid properties on the vapor ingestion phenomenon and comparisons of vapor ingestion heights for both environments are also presented.

INTRODUCTION

As space missions become increasingly ambitious, efficient use of onboard, stored liquids becomes vital. Indeed, sufficiently long-term space flights may require "refueling" of systems such as vehicle propellant tanks, reaction control system tanks, and life-support subsystems. For all such spacecraft whether the vehicles are powered by chemical, solid, or nuclear means, the efficient use of liquids requires the predetermined knowledge of the behavior of the liquid-vapor interface during outflow at reduced gravity.

A detailed program is well under way at Lewis in which the dynamic behavior of liquids during outflow from containers is being studied in weightless and reduced-gravity environments. An initial study was performed by Nussle and is reported in reference 1. Two significant results can be inferred from this study: (1) the amount of liquid expelled before vapor was ingested in the outlet line was a strong function of outflow velocity, and (2) baffling the pressurant inlet port eliminated direct impingement of the incoming gas on the liquid surface and resulted in considerably reduced liquid residuals. Derdul then performed an investigation studying the behavior of the liquid-vapor interface during

outflow. This study (ref. 2) resulted in the correlation of the interface distortion with Weber number. (The Weber number is a dimensionless quantity relating the inertia to capillary forces.) Grubb then reported in reference 3 the results of an investigation of the behavior of the liquid-vapor interface after termination of outflow.

Although some studies of vapor ingestion may be found in the literature, none were performed in a weightless environment. Gluck, et al., (ref. 4) correlated vapor ingestion heights using the Froude number by conducting a series of experiments at normal gravity. (The Froude number is a nondimensional ratio of inertia to gravitational forces.) Lubin and Hurwitz (ref. 5) developed an analysis for vapor ingestion which resulted in a modified Froude number, and accompanying experimental tests substantiated the theory. These correlating relations, however, were not readily amenable to the case of vapor ingestion in weightlessness. The analysis of reference 6 modified the theory of reference 5 to include an estimate of the surface-tension effect during draining. The resulting expression for the critical height at vapor ingestion, when solved for weightlessness, predicted a dependence on the Weber number.

This report presents the results of an experimental study of vapor ingestion in normal-gravity and weightless environments. The tests were conducted at the Lewis Research Center's 2.2-Second Zero-Gravity Facility. The experiment containers were flat-bottom, cylindrical tanks, each containing a cylindrical drain.

SYMBOLS

g	acceleration due to gravity, 980 cm/sec^2
h_{cr}	critical height, cm
h_i	initial liquid height, cm
h_{vi}	vapor ingestion height, cm
Q_o	outflow rate, cm^3/sec
R	tank radius, cm
r_o	outlet radius, cm
V_o	outflow velocity (liquid velocity in outlet line), cm/sec
β	specific surface tension, σ/ρ, cm^3/sec^2
μ	absolute viscosity, cP
ρ	density, g/cm^3
σ	surface tension, dynes/cm

APPARATUS AND PROCEDURE

A detailed description of the 2.2-Second Zero-Gravity Facility and the experiment apparatus and procedure used are given in the appendix. Briefly, the experimental investigation utilized two flat-bottom, cylindrical tanks, 2 and 4 centimeters in radius. Each tank was fitted with cylindrical outlet lines equal to one-tenth and one-twentieth of the respective tank radii. Details of the tank designs are also presented in the appendix. The draining phenomenon was recorded on film for a range of liquid heights and outflow rates in both normal gravity and weightlessness. Outflow was achieved by means of a pressurization technique also described in the appendix.

Three liquids were chosen for this study and are listed in table I along with pertinent liquid properties. To improve the quality of the photographic data, a small amount of dye was added to the test liquids. Addition of this dye has no measurable effect on the liquid properties.

TABLE I. - PROPERTIES OF TEST LIQUIDS

[Contact angle with cast acrylic plastic in air, 0°.]

Liquid	Surface tension at 20° C, σ, dynes/cm	Density at 20° C, ρ, g/cm^3	Viscosity at 20° C, μ, cP	Specific surface tension, β, cm^3/sec^2
Ethanol	22.3	0.789	1.2	28.3
Trichloro-trifluoro-ethane	18.6	1.58	.7	11.8
60 Ethanol - 40 glycerol (percent by volume)	26.9	.988	15.4	27.2

DESCRIPTION OF VAPOR INGESTION PHENOMENON

During tank draining there exists a time when the center of the liquid-vapor interface is suddenly drawn toward the outlet. At this time, a dip in the liquid-vapor interface forms above the drain and rapidly accelerates toward the outlet, followed quickly by ingestion of vapor into the outlet line. This phenomenon is illustrated for both normal gravity and weightlessness in figure 1. The sketches in the figure indicate the interface shape during draining while the displacement-time graphs show the interface height as a function of draining time.

In normal gravity (fig. 1(a)), the interface remains essentially flat while draining at constant velocity until the incipience of vapor ingestion when a dip forms at the center of the liquid-vapor interface. The dip then rapidly accelerates toward the outlet, followed by ingestion of vapor into the drain line. The interface shape away from the drain remains essentially flat, even at the time of vapor ingestion, as shown in the sketch. The displacement-time graph shows the rapid acceleration of the interface centerline towards the outlet and at the same time depicts the liquid-vapor interface height away from the drain. At vapor ingestion, this interface height away from the drain, where the interface is flat, is denoted as the vapor ingestion height. The height of the liquid-vapor interface at the incipience of vapor ingestion (at the time the dip forms) is called the critical height.

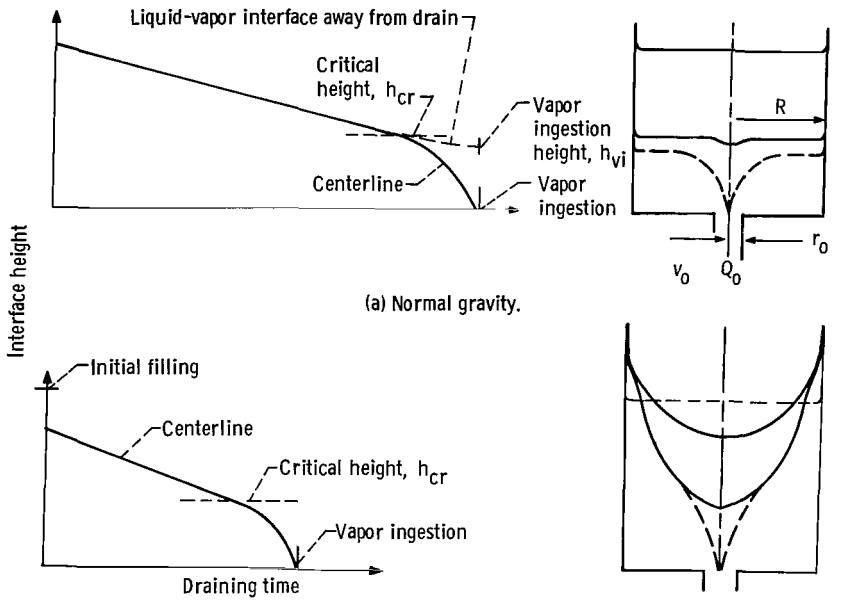

Figure 1. - Vapor ingestion phenomenon.

In order to adequately define the vapor ingestion phenomenon, knowledge of either the incipience of vapor ingestion (critical height) or vapor ingestion height is necessary. The analysis of reference 5 mathematically derived a vapor ingestion height measured away from the drain as a function of Froude number in terms of outflow rate and outlet radius. This criterion is meaningful for draining in normal gravity in which (as described earlier) the moving interface remains flat away from the drain. As a comparison with the theoretical analysis, supporting experimental data were presented in reference 5. In describing the vapor ingestion phenomenon in normal gravity, therefore, the vapor ingestion height away from the drain is used.

The draining phenomenon in weightlessness is similar to that in normal gravity. The shape of the liquid-vapor interface is considerably different, however, as shown in the sketch of figure 1(b). In weightlessness, the interface prior to draining is a curved surface whose shape is determined by surface tension and liquid-to-solid contact angle. During draining, the interface distorts from this initially curved surface (ref. 2). As in normal gravity, the interface centerline height moves at constant velocity until incipience of vapor ingestion and then accelerates into the outlet. Again, the critical height is defined as the liquid-vapor-interface height at the time of incipience of vapor ingestion. For both normal gravity and weightlessness, the critical height occurs at the time when the interface centerline deviates from constant-velocity draining (see fig. 1). However, in zero gravity, the interface height away from the drain is everywhere different because of the highly curved liquid-vapor interface shape. In describing the vapor ingestion phenomenon in weightlessness, therefore, the critical height is used and is measured directly over the drain.

The phenomenon, for both normal gravity and weightlessness, is illustrated in the photographic sequences in figure 2 for typical draining cases. The first photograph in each sequence depicts the initial interface shape. As discussed later (p. 11), the weightless experiments were performed by allowing sufficient time for the liquid-vapor-interface centerline to reach its low point prior to initiation of draining. This configuration, as shown, is nearly hemispherical in shape, compared to the flat interface at normal gravity. During draining in normal gravity (fig. 2(a-2)), the interface remains flat. However, in weightlessness (fig. 2(b-2)), the interface distorts during outflow with a considerable amount of liquid remaining on the tank wall. The shapes are also shown at the time the interface reaches the incipience of vapor ingestion (figs. 2(a-3) and (b-3)) and at the instant vapor is ingested in the drain (figs. 2(a-4) and (b-4)).

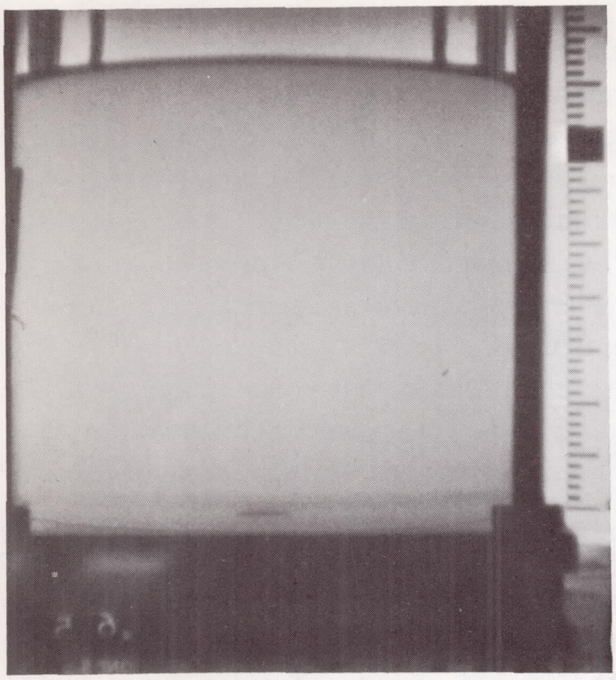

(a-1) Initiation of draining.

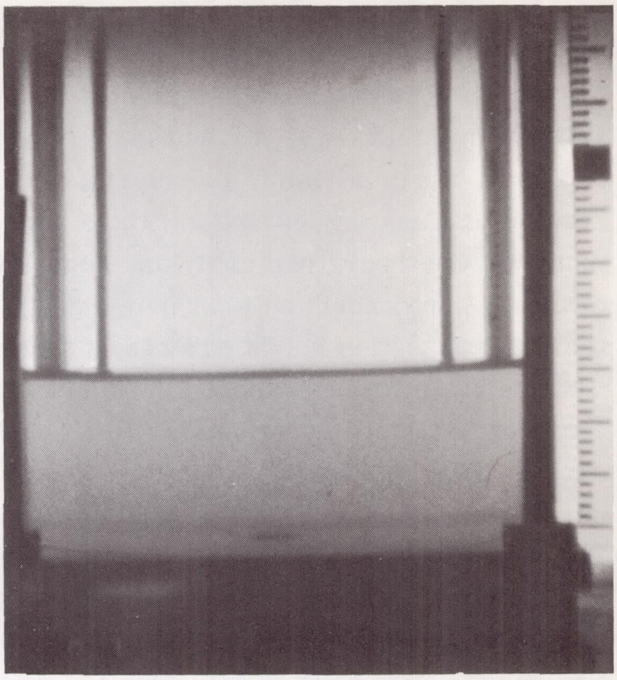

(a-2) Interface shape during draining.

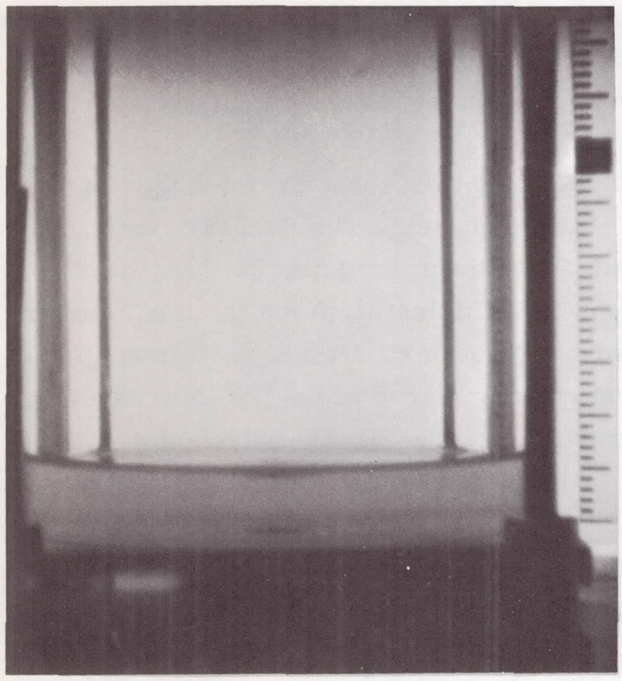

(a-3) Incipience of vapor ingestion.

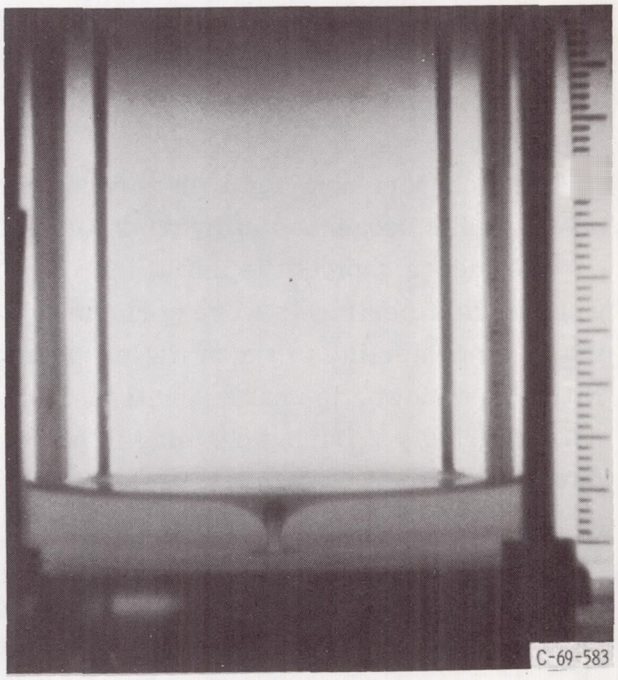

(a-4) Vapor ingestion.

(a) Normal gravity.

Figure 2. - Photographic sequence illustrating vapor ingestion phenomenon in both normal gravity and weightlessness.

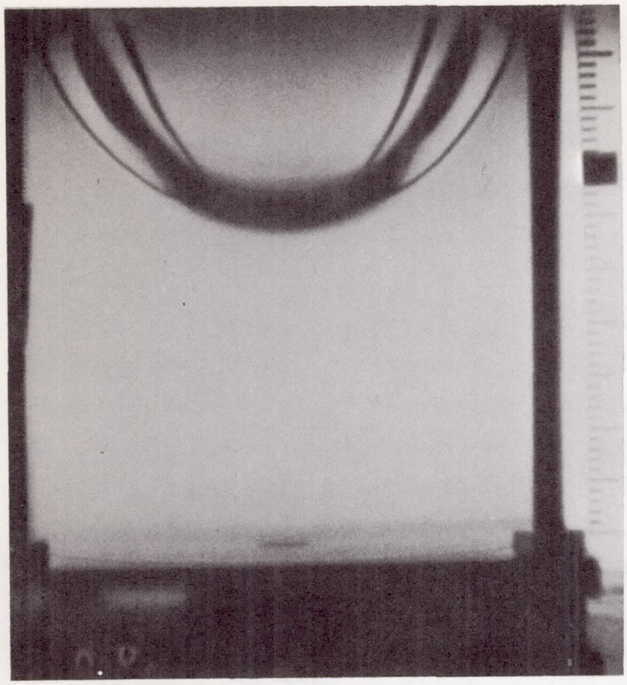

(b-1) Initiation of draining.

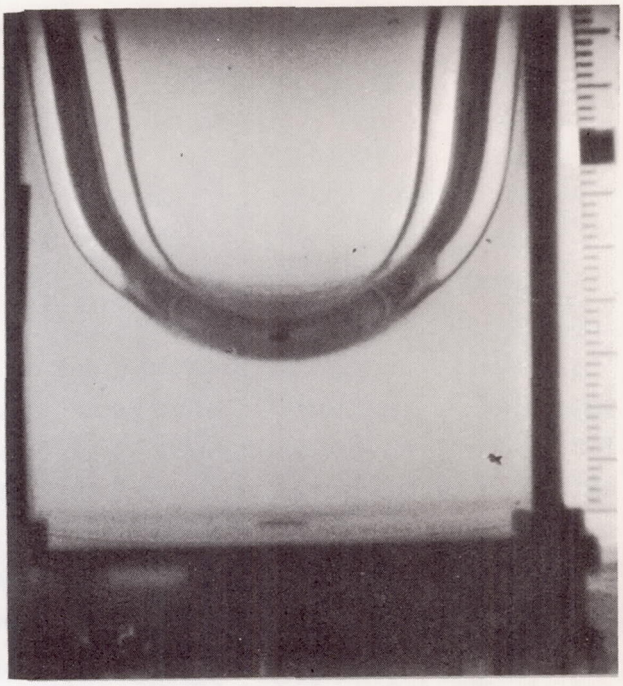

(b-2) Interface shape during draining.

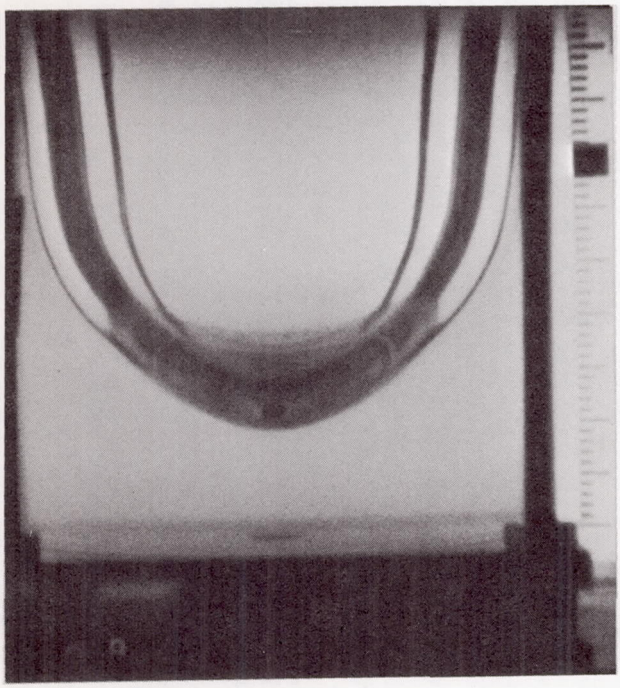

(b-3) Incipience of vapor ingestion.

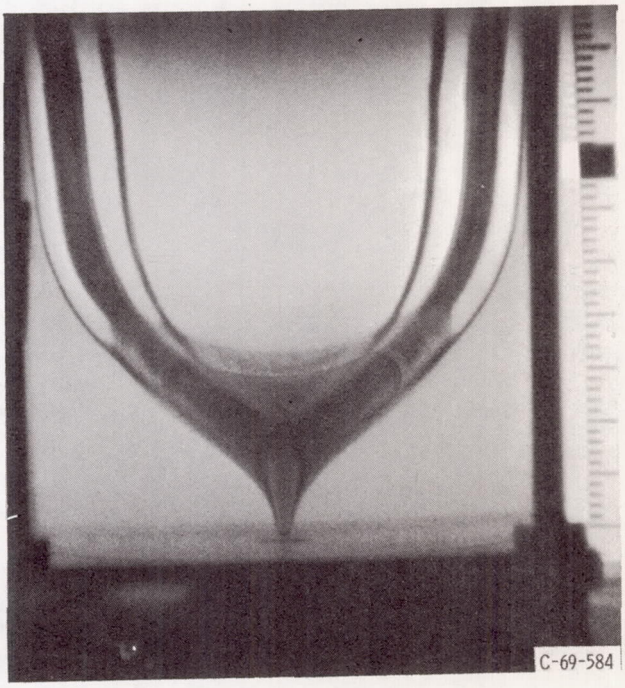

(b-4) Vapor ingestion.

(b) Weightlessness.

Figure 2. - Concluded.

RESULTS AND DISCUSSION

Vapor Ingestion in Normal Gravity

Experimental data were obtained for tank sizes of 2 and 4 centimeters in radius. Each tank was fitted with cylindrical outlet lines equal to one-tenth and one-twentieth of the respective tank radii. The flat-bottom tanks for each of these tests were filled to a liquid height of 2 tank radii. Displacement-time draining curves, similar to those of figure 1(a), showing interface height as a function of draining time were plotted from the data film for each outflow test. Representative draining curves are presented in figure 3 for the 2-centimeter-radius tank, with 0.1-centimeter-radius outlet. Computation of the outflow velocities shown in figure 3 was based on the constant interface velocity within the tank (taken from the draining curves) and the area ratio of tank cross section to outlet cross section. As described in the previous section, outflow at normal gravity is characterized by a flat interface draining at constant velocity until the critical height is reached. Thereupon a dip forms at the center of the liquid-vapor interface. The dip accelerates toward the outlet, as shown by the curves in figure 3. The interface away from the drain (depicted by tailed symbols) continues to move at a slightly lower rate, since the liquid drained from the tank was being removed primarily from the liquid directly above the outlet. The vapor ingestion height, as described earlier, is the liquid-vapor interface height away from the drain at the instant vapor enters into the outlet line. Both the critical heights and the vapor ingestion heights are indicated in figure 3.

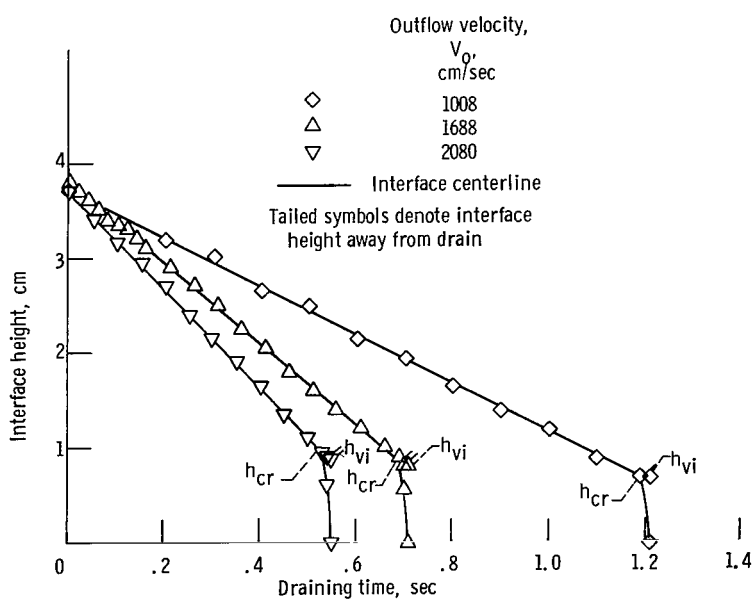

Figure 3. - Representative draining curves. Normal gravity; tank radius, 2 centimeters; outlet radius, 0.1 centimeter; liquid, ethanol.

The vapor ingestion heights obtained from each draining test were plotted (in log-log form) as a function of outflow velocity in figure 4. The data in this figure indicate a strong dependence of vapor ingestion height on both the outflow velocity and the outlet size, and an independence of tank size and liquid properties. The analysis of reference 5 for low-viscosity liquids predicted this dependence for draining cases in which the vapor ingestion height is large compared to the outlet radius. The Froude number as derived in reference 5 for these conditions is

$$\frac{Q_o^2}{g r_o^2 h_{vi}^3} = \frac{6.5}{\left(\frac{r_o}{h_{vi}}\right)^2} \qquad (1)$$

where $r_o/h_{vi} \ll 1.0$.

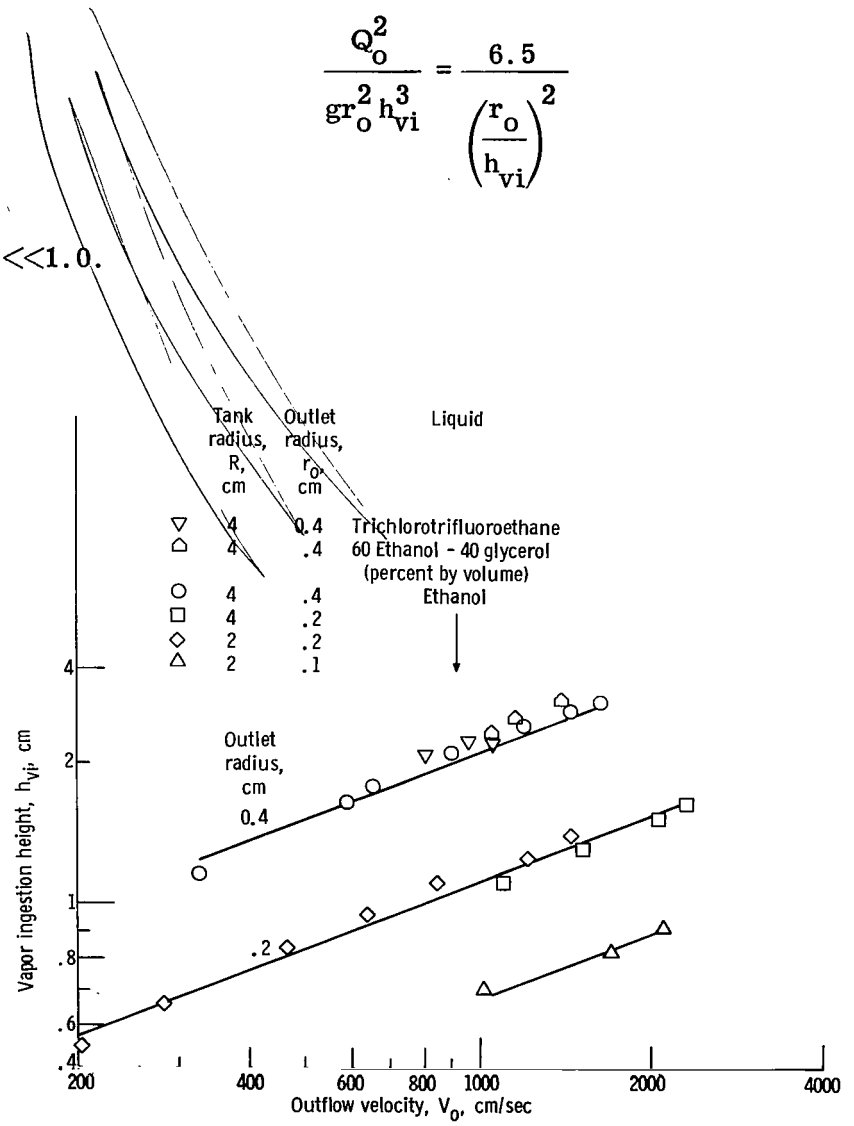

Figure 4. - Vapor ingestion heights in normal gravity. Initial liquid height, 2 tank radii.

Simplifying equation (1) and nondimensionalizing using the tank radius R (in order to compare with the weightlessness results given in the next section) yields the following expression:

$$\frac{Q_o^2}{gR^5} = 6.5\left(\frac{h_{vi}}{R}\right)^5 \tag{2}$$

where $r_o/h_{vi} \ll 1.0$. The expression derived in equation (2), therefore, provides a convenient form for comparing the experimental data of this investigation with the theoretical analysis of reference 5. This comparison is shown in figure 5, with the limiting expression of equation (2) superimposed on the graph. The experimental results agree favorably with the theoretical curve. The data show better agreement at the higher Froude numbers than at the lower values. This result is expected because of the constraint placed on the analytical expression, which is that the vapor ingestion height be large compared to the outlet radius. The lowest value of vapor ingestion height was approximately three times the outlet radius (note fig. 4), indicating good agreement with the theory for $r_o/h_{vi} < 1/3$.

The range of liquid properties over which data were obtained varied from 0.7 to 15.4 centipoise for viscosity and from 11.8 to 28.3 cubic centimeters per square second for specific surface tension. Data for trichlorotrifluoroethane and a mixture of 60 percent ethanol with 40 percent glycerol, by volume, were compared with the data for ethanol. Of significance is the fact that no effect of liquid properties was noticeable over the ranges tested (see fig. 5).

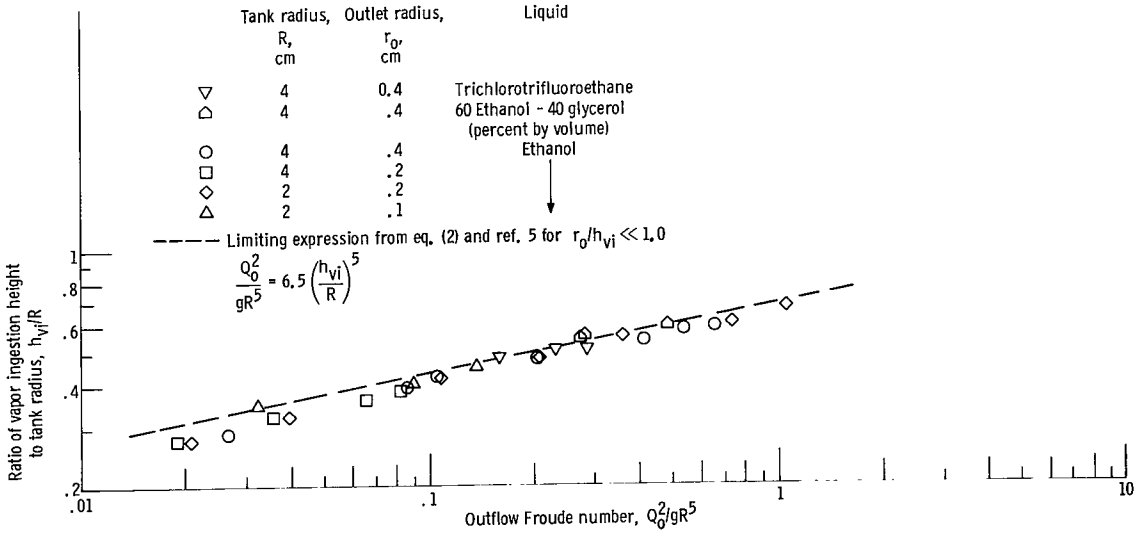

Figure 5. - Prediction of vapor ingestion height in normal gravity by outflow Froude relation. Initial liquid height, 2 tank radii.

Vapor Ingestion in Weightlessness

Experimental data were obtained in a weightless environment for a similar range of tank radii, outlet sizes, drain rates, and liquids. The flat-bottom tanks were initially filled with liquid to a height of 2 tank radii. Upon entering weightlessness, the liquid-vapor interface forms into a curved interface, as already discussed. Since the time required for the interface to come to static equilibrium was too long to permit a draining test to follow, the initiation of outflow was implemented at the time when the interface centerline reached its low point. The interface centerline velocity at this time is zero. This procedure was similar to that of reference 2. Typical draining curves for the weightless tests, as shown in figure 6, therefore, indicate draining from an interface

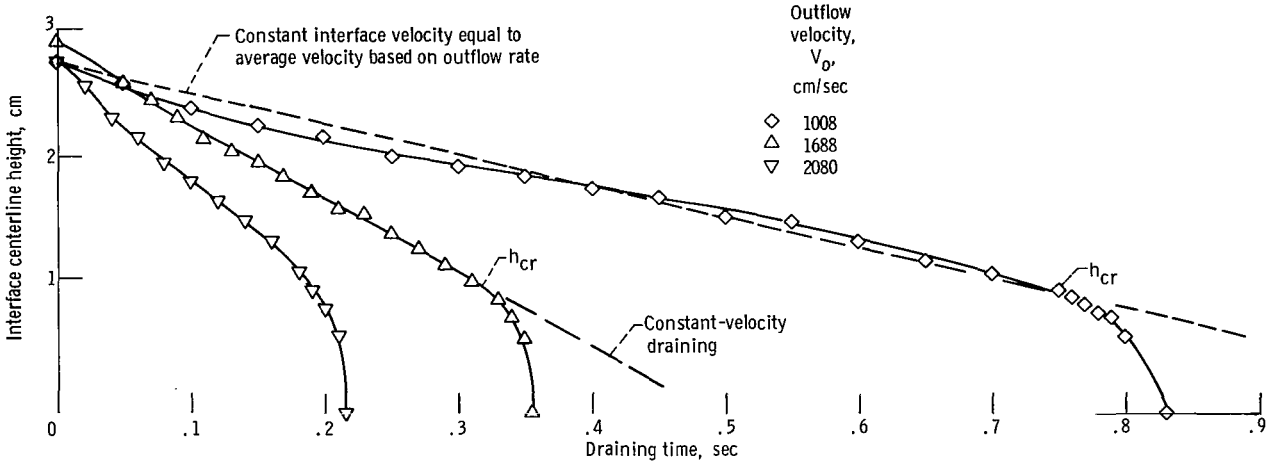

Figure 6. - Representative draining curves in weightlessness. Tank radius, 2 centimeters; outlet radius, 0.1 centimeter; liquid, ethanol.

height initially at a level somewhat less than 2 tank radii. The examples shown are, again, for the 2-centimeter-radius tank with a 0.1-centimeter-radius outlet, for the same three outflow velocities. After a short startup transient, the liquid-vapor interface along the tank centerline, in general, shows draining at constant velocity, followed by acceleration toward the drain. The constant-velocity line appears in figure 6 as a dashed line. A typical critical height is also denoted.

A few exceptions to constant-velocity draining occurred at the lowest outflow velocities. Here the interface oscillated very slowly in the case shown in figure 6, or as in other cases, the interface centerline remained at a constant height for a considerable length of time while liquid drained from the tank. Since draining was initiated at a preset time for each zero-gravity test, the interface at the instant of outflow may not

have been precisely at the low point. When draining at very low interface velocities, the interface is moving so slowly that the motion of the interface due to interface formation may still be observed. Furthermore, the draining curves were obtained only for the interface centerline and do not describe the motion of the complete interface. Study of the motion picture film for these cases showed that the interface away from the centerline was moving downward when the center of the interface remained stationary. At these times the interface shape tended to flatten.

For these cases, where the liquid-vapor interface velocity approached the average interface velocity in the tank, the average velocity was used to determine the critical height. The study of reference 2 shows that at low Weber numbers (low drain rates) the interface distortion, which relates the deviation of centerline velocity from the mean, approaches zero. The average interface velocity, then, is superimposed on the actual draining curve starting with the initiation of outflow, as shown in figure 6. Therefore, the critical height, for these cases in which the interface velocity is very low, was the interface centerline height at which the draining curve intersects the average line nearest the outlet. An example is shown in figure 6 for an outflow velocity of 1008 centimeters per second.

The critical heights obtained for each configuration were plotted in log-log form as a function of the outflow velocity in figure 7. The data show that the critical height increases with increasing draining rate; however, the dependence is not as strong as for the normal-gravity outflow (fig. 4). Figure 7 also indicates effects of tank and outlet

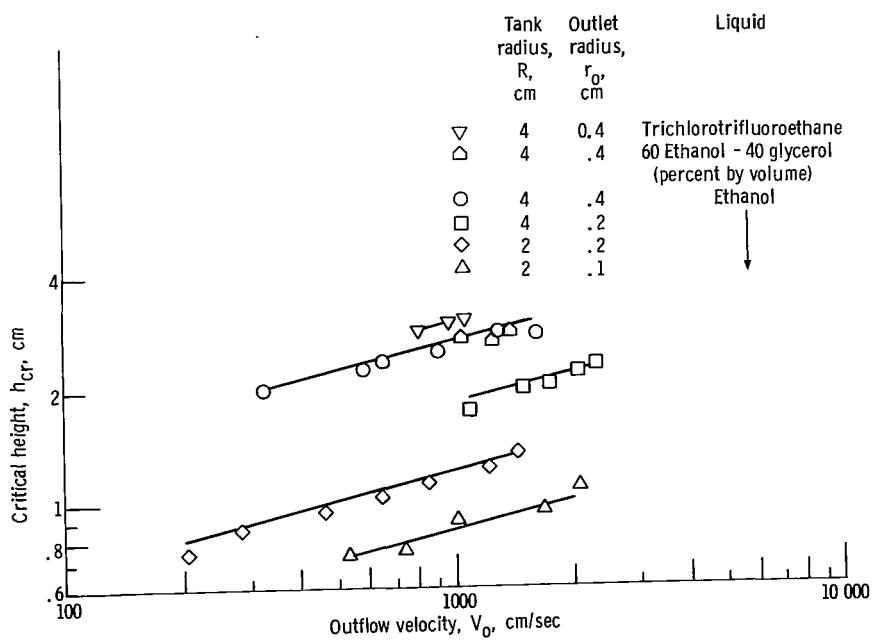

Figure 7. - Critical heights in weightlessness.

size and specific surface tension. The analysis of reference 6, which includes an estimate of the effect of surface tension on the draining phenomenon, predicts a dependence on Weber number for outflow in weightlessness. When the data of figure 7 were replotted by nondimensionalizing the critical height with the tank radius and the velocity by means of the outflow Weber number, excellent correlation of the critical height with Weber number occurred (fig. 8). The resulting Weber number correlation, shown by the line in figure 8, may be expressed as follows:

$$\frac{Q_o^2}{\beta R^3} = 4000\left(\frac{h_{cr}}{R}\right)^8$$

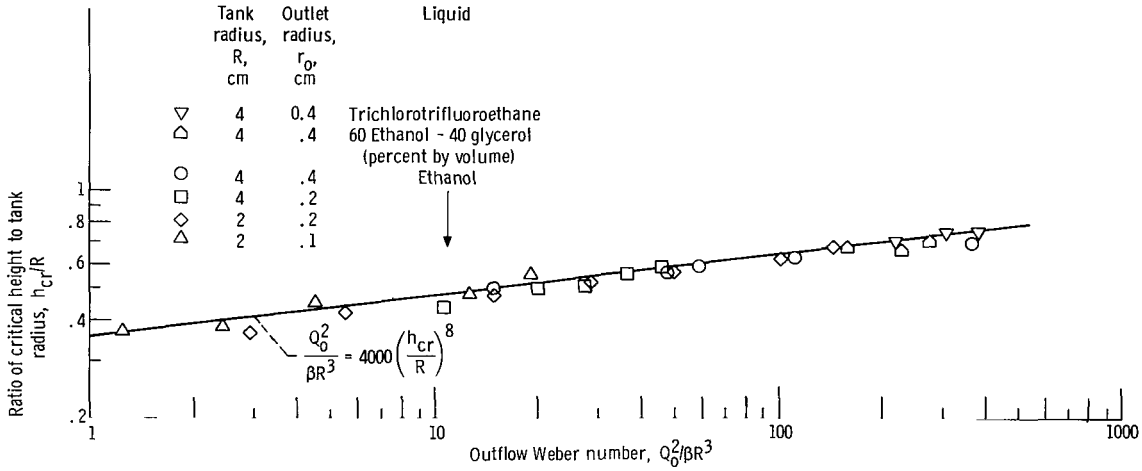

Figure 8. - Prediction of incipience of vapor ingestion in weightlessness by outflow Weber number. Initial liquid height, 2 tank radii.

Comparison of Vapor Ingestion in Normal Gravity and Weightlessness

Normal-gravity experimental results have been presented, and they agree with the theoretical analysis of reference 5, in which the vapor ingestion phenomenon was correlated by Froude number. For the same conditions, results for similar tests in a weightless environment have also been obtained. In weightlessness, the vapor ingestion phenomenon was shown to be correlated by the Weber number as anticipated from the surface-tension analysis of reference 6. Intuitively, the relation between the phenomenon in weightlessness and in normal gravity should be the Bond number (ratio of Weber and Froude numbers). Using the slopes of the correlating relations as the exponential, the respective vapor ingestion heights are indeed shown to be Bond number dependent in figure 9. Here the critical height in weightlessness is plotted as a function of the vapor

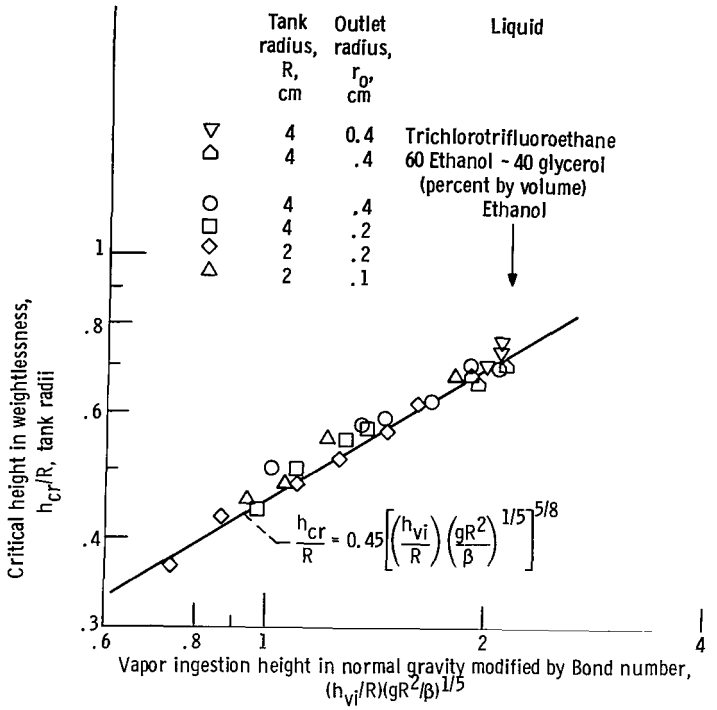

Figure 9. - Comparison of vapor ingestion in normal gravity and weightlessness. Initial liquid height, 2 tank radii.

ingestion height in normal gravity modified by the Bond number to the 1/5 power. The Bond number is the value calculated for normal gravity; that is, the g term is the acceleration at normal gravity. The data presented are limited to initial liquid height of 2 tank radii. The line representing the data was obtained by equating the outflow rates for the respective correlating expressions for normal gravity and weightlessness. This expression is

$$\frac{h_{cr}}{R} = 0.45\left[\left(\frac{h_{vi}}{R}\right)\left(\frac{gR^2}{\beta}\right)^{1/5}\right]^{5/8}$$

The usefulness of this vapor ingestion comparison is that the relative heights in both environments may be compared for the same draining conditions regardless of tank size or liquid. In order to directly compare actual heights in weightlessness and normal gravity, the vapor ingestion correlation in figure 9 was used to calculate vapor ingestion heights for a range of tank sizes. The results, shown in figure 10, compare directly

the critical height in weightlessness with the normal-gravity vapor ingestion height. The tank sizes presented range from 2 to 330 centimeters (~ 1 in. to 10.8 ft) in radius and were calculated for a filling level of 2 tank radii with liquid hydrogen (β equal to 30 cm^3/sec^2 was used). The lower limits shown for each tank size are the nominal vapor ingestion heights below which a deviation from the 1/5-power Froude correlation ($r_o/h_{vi} < 1/3$) becomes significant. Use of this normal-gravity - weightlessness comparison figure below these values introduces increasing error for decreasing vapor ingestion heights. To compare data in this regime the normal-gravity vapor ingestion height should be determined from the theoretical curves contained in reference 2 or by experimentation. The vapor ingestion height may then be compared with the critical height in weightlessness from figure 8 for the same outflow rate. The upper limits reflect the obvious restrictions caused by the initial liquid height.

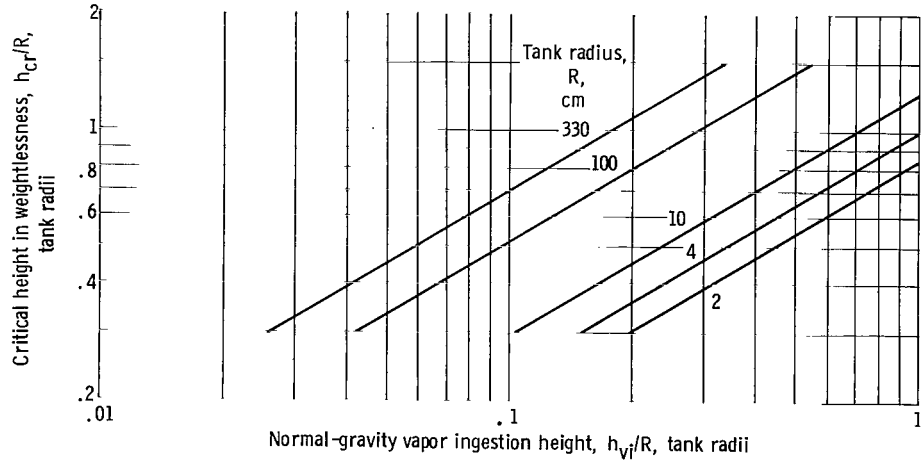

Figure 10. - Vapor ingestion comparison calculated for various tanks filled to a level of 2 tank radii with liquid hydrogen.

For comparisons over the ranges presented, the curves of figure 10 may be used directly. As an example, if the vapor ingestion height for a known flow rate in a 2-centimeter-radius, flat-bottom tank is 0.5 R (1.0 cm), the critical height for draining in weightlessness at that same flow rate is 0.54 R (1.08 cm) above the outlet. For a tank whose radius is 330 centimeters and in which the vapor ingestion height is one-tenth the tank radius, the critical height in weightlessness is estimated to be 0.7 R. As these two examples show, the critical height in weightlessness is generally higher than the

vapor ingestion height in normal gravity for corresponding draining conditions and tank size.

Effect of Draining on Liquid Residuals

When the incipience of vapor ingestion is known, ingestion of vapor into feed lines or vulnerable pumping systems may be delayed by reducing the draining rate at the proper time during the draining process. A reduction in drain rate, or throttling, lowers the Froude number in normal gravity or the Weber number in weightlessness, which, in turn, lowers the height at which vapor ingestion occurs. Of particular importance is the liquid residual in the tank at the termination of draining. As a matter of definition for this report, draining is considered terminated at the instant vapor reaches the outlet, although liquid with entrained vapor may be continually drawn from the tank until the liquid is depleted. The liquid residual, therefore, is the amount of liquid remaining in the tank at the instant of vapor ingestion in the outlet. The liquid residuals for all the tests presented herein were easily obtainable by means of the draining curves. The curves yielded the draining time, and with this and the outflow rate for each drain case, the total volume of liquid drained was calculated. The liquid residuals were obtained by subtracting the volume of liquid drained from the initial liquid volume.

The results of these calculations are presented in nondimensional form as residual fractions in figure 11. The residual fraction is the ratio of residual liquid volume at the time of vapor ingestion to the initial liquid volume. The residual fractions are shown as a function of the correlating Froude number in normal gravity (fig. 11(a)), and as a function of correlating Weber number in weightlessness (fig. 11(b)). In figure 11(c), the residuals for normal gravity and weightlessness for identical conditions are compared using a ratio of Froude and Weber numbers. The data in figure 11 are limited to the constant liquid height of 2 tank radii.

The residual fraction in normal gravity increases with increasing Froude number. This increase is proportional to the vapor ingestion height. In weightlessness, however, the residual fraction increases with increasing Weber number over a narrow range. Above a Weber number of approximately 25, the residual fraction remained level at values near 0.70 to 0.75. This is primarily a result of the highly curved shape of the interface during draining in weightlessness. At low flow rates, the interface is nearly hemispherical. As the flow rate increases, the interface distorts considerably from the already hemispherical shape (ref. 2), until a constant value of distortion is reached.

The residuals in weightlessness are compared with those for normal-gravity draining by plotting the ratios of the coordinates in figures 11(a) and (b) for equal outflow rates. The resulting curve in figure 11(c) clearly indicates that, for the same conditions,

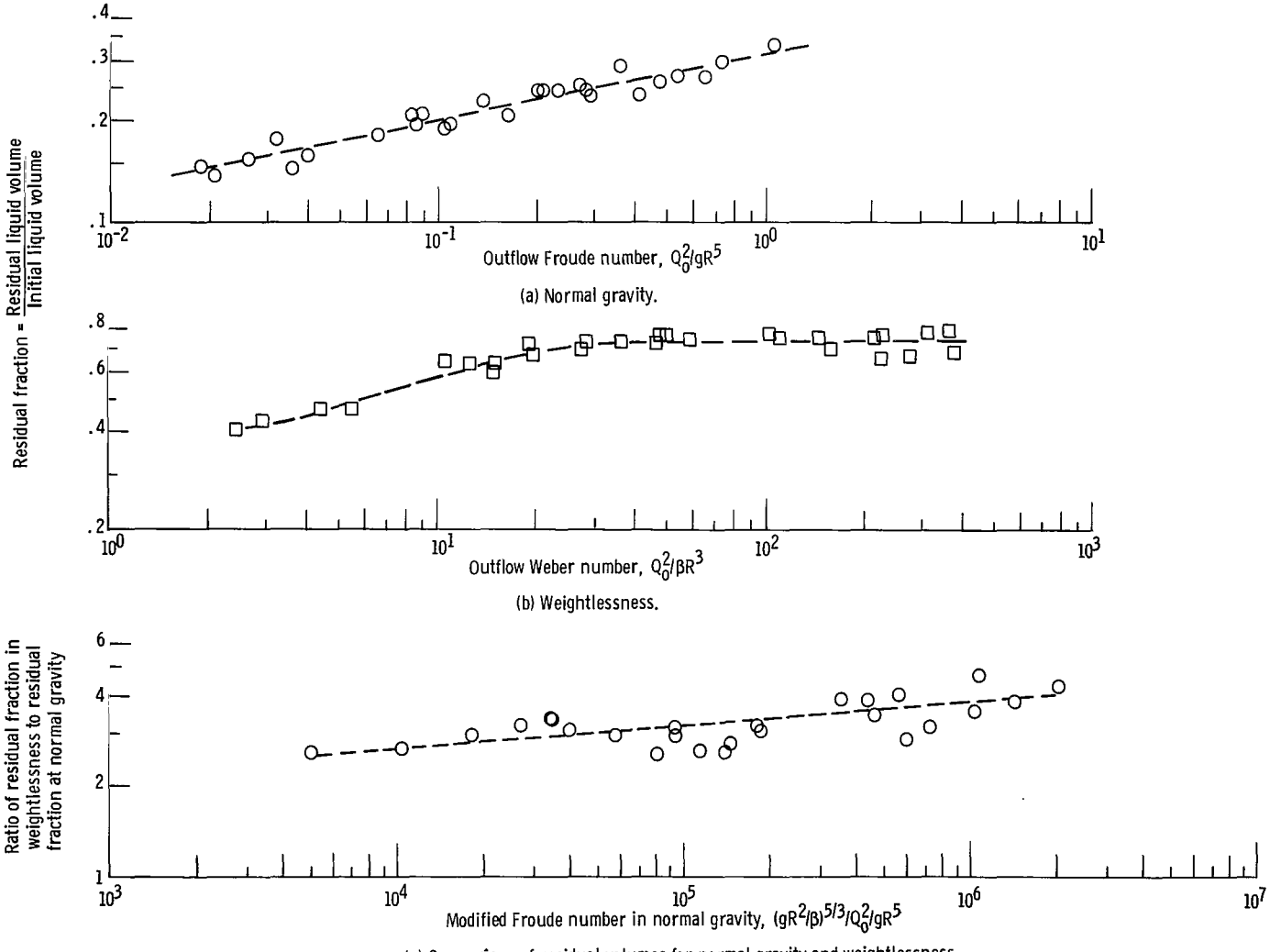

Figure 11. - Residual fractions in normal gravity and weightlessness. Initial fill height, 2 tank radii.

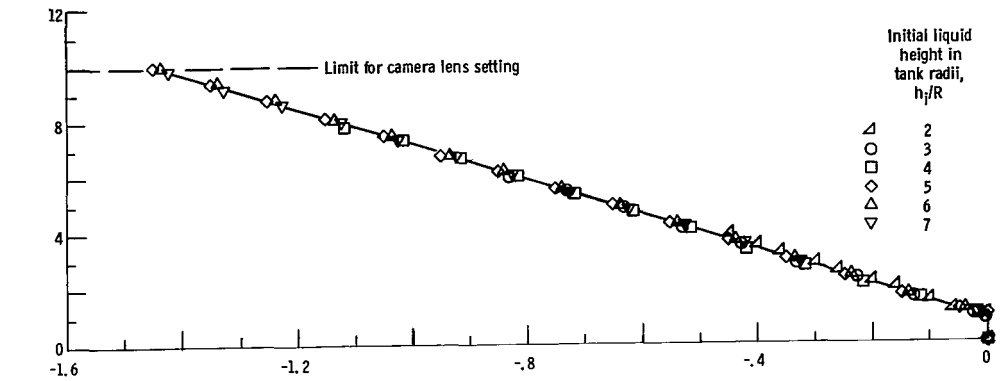

(a-1) Outflow velocity, 638 centimeters per second.

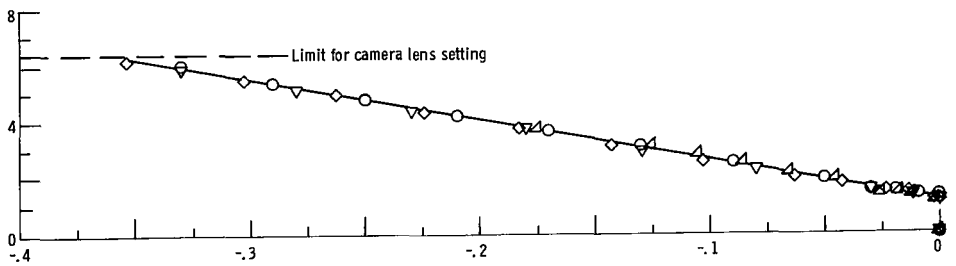

(a-2) Outflow velocity, 1440 centimeters per second.

(a) Normal gravity.

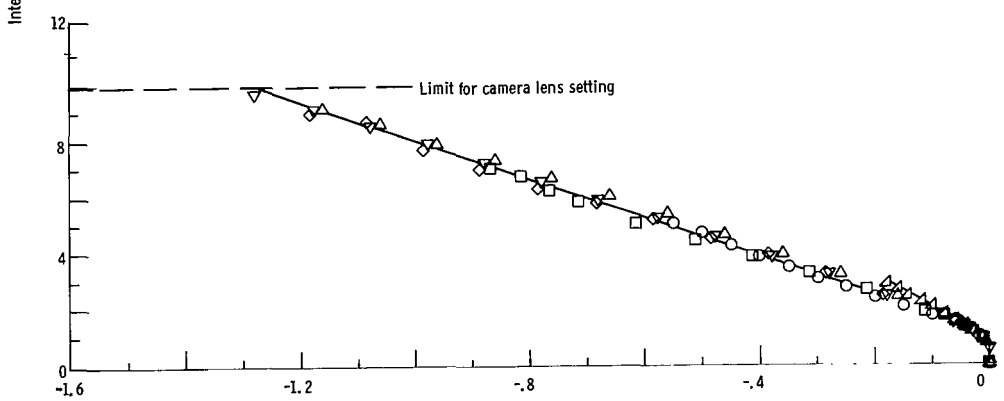

(b-1) Outflow velocity, 638 centimeters per second.

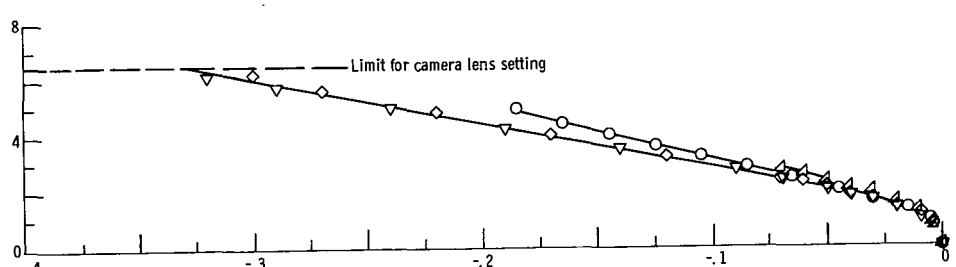

(b-2) Outflow velocity, 1440 centimeters per second.

(b) Weightlessness.

Interface height, cm

Figure 12. - Draining curves as function of initial liquid height. Tank radius, 2 centimeters; outlet radius, 0.2 centimeter; liquid, ethanol.

the residuals in weightlessness are considerably higher than the residuals in normal gravity (at least two to four times for the range of outflow rates investigated). The higher residuals in weightlessness, however, are partly due to the naturally curved interface and to the flat-bottom tank.

Effect of Initial Liquid Height

In order to determine whether the initial liquid height affected the vapor ingestion phenomenon, the 2-centimeter-radius tank with the 0.2-centimeter-radius outlet was subjected to a series of draining tests using ethanol, in which the initial liquid height was varied from 2 to 7 tank radii. Two previously tested outflow rates were selected: a relatively low value corresponding to an outflow velocity of 638 centimeters per second and a high value corresponding to an outflow velocity of 1440 centimeters per second. The draining curves for these tests in normal gravity are shown in figure 12(a). The figure clearly shows no effect of initial liquid height in normal gravity for either of the two rates. Furthermore, for each drain rate, regardless of initial liquid height, the vapor ingestion height remained constant.

The draining curves in weightlessness are shown in figure 12(b), and indicate very little, if any, effect of initial liquid height on the vapor ingestion phenomenon under weightless conditions. This result appears to validate the Weber number correlation in weightlessness independent of initial liquid height (for heights of 2 tank radii and greater). Also, as figure 12(b) shows, there is a small effect of initial height on the interface centerline velocity; the effect is more apparent at the lower initial heights and at the higher outflow velocity. This effect on the interface centerline velocity agrees with the interface distortion study of reference 2, in which the liquid-vapor-interface distortion was shown to increase with decreasing initial liquid height.

SUMMARY OF RESULTS

An experimental program was conducted to study the vapor ingestion phenomenon in both normal gravity and weightlessness during draining from flat-bottom cylindrical tanks. Tanks used for the tests were 2 and 4 centimeters in radius. Results were obtained over a range of outlet sizes, flow rates, liquid properties, and initial liquid heights. For the ranges investigated, the results may be summarized as follows:

1. The analysis of Lubin and Hurwitz (ref. 5) predicting vapor ingestion in normal gravity by means of the Froude number was correlated with the experimental data of this investigation for low-viscosity liquids. Increasing the viscosity from 0.7 to

15.4 centipoise had no noticeable effect on the vapor ingestion phenomenon.

2. In weightlessness, the critical liquid height, defined as the liquid-vapor interface centerline height at the incipience of vapor ingestion, was correlated by the Weber number relation $Q_o^2/\beta R^3 = 4000\,(h_{cr}/R)^8$ where Q_o is the outflow rate, β is specific surface tension, R is tank radius, and h_{cr} is the critical height.

3. Although tank size has no effect at normal gravity, it does affect the vapor ingestion phenomenon in weightlessness.

4. The critical height in weightlessness is generally higher than the vapor ingestion height in normal gravity for identical conditions.

5. For the same conditions, the liquid residuals, at the time of vapor ingestion after draining in weightlessness, are considerably higher than the residuals in normal gravity. The range varied from two to four times, over the outflow rates investigated. The higher residuals in weightlessness were partially a result of the combination of naturally curved liquid-vapor interface and the flat-bottom tank.

6. A change of inital liquid height ranging from 2 to 7 tank radii had little or no effect on the vapor ingestion phenomenon either at normal gravity or in weightlessness.

Lewis Research Center,
National Aeronautics and Space Administration,
Cleveland, Ohio, January 31, 1969,
124-09-17-01-22.

APPENDIX - APPARATUS AND PROCEDURE

Test Facility

The experimental data for this study were obtained in the Lewis Research Center's 2.2-Second Zero-Gravity Facility. A schematic diagram of this facility is shown in figure 13. The facility consists of a building 6.4 meters (21 ft) square by 30.5 meters (100 ft) tall. Contained within the building is a drop area 27 meters (89 ft) long with a cross section 1.5 by 2.75 meters (5 by 9 ft).

The service building has, as its major elements, a shop and service area, a calibration room, and a controlled environment room. Those components of the experiment which require special handling are prepared in the facility's controlled environment room. This air-conditioned and filtered room (shown in fig. 14) contains an ultrasonic cleaning system and the laboratory equipment necessary for handling test liquids.

Mode of operation. - A 2.2-second period of weightlessness is obtained by allowing the experiment package to free fall from the top of the drop area. In order to minimize drag on the experiment package, it is enclosed in a drag shield, designed with a high ratio of weight to frontal area and a low drag coefficient. The relative motion of the experiment package with respect to the drag shield during a test is shown in figure 15. Throughout the test the experiment package and drag shield fall freely and independently of each other; that is, no guide wires, electrical lines, etc., are connected to either. Therefore, the only force acting on the freely falling experiment package is the air drag associated with the relative motion of the package within the enclosure of the drag shield. This air drag results in an equivalent gravitational acceleration acting on the experiment, which is estimated to be below 10^{-5} g's.

Release system. - The experiment package, installed within the drag shield, is suspended at the top of the drop area by means of a highly stressed music wire attached to the release system. This release system consists of a double-acting air cylinder with a hard-steel knife edge attached to the piston. Pressurization of the air cylinder drives the knife edge against the wire which is backed by an anvil. The resulting notch causes the wire to fail, smoothly releasing the experiment. No measurable disturbances are imparted to the package by this release procedure.

Recovery system. - After the experiment package and drag shield have traversed the total length of the drop area, they are recovered by decelerating in a 2.2-meter- (7-ft-) deep container filled with sand. The deceleration rate (averaging 15 g's) is controlled by selectively varying the tips of the deceleration spikes mounted on the bottom of the drag shield (fig. 13). At the time of impact of the drag shield in the

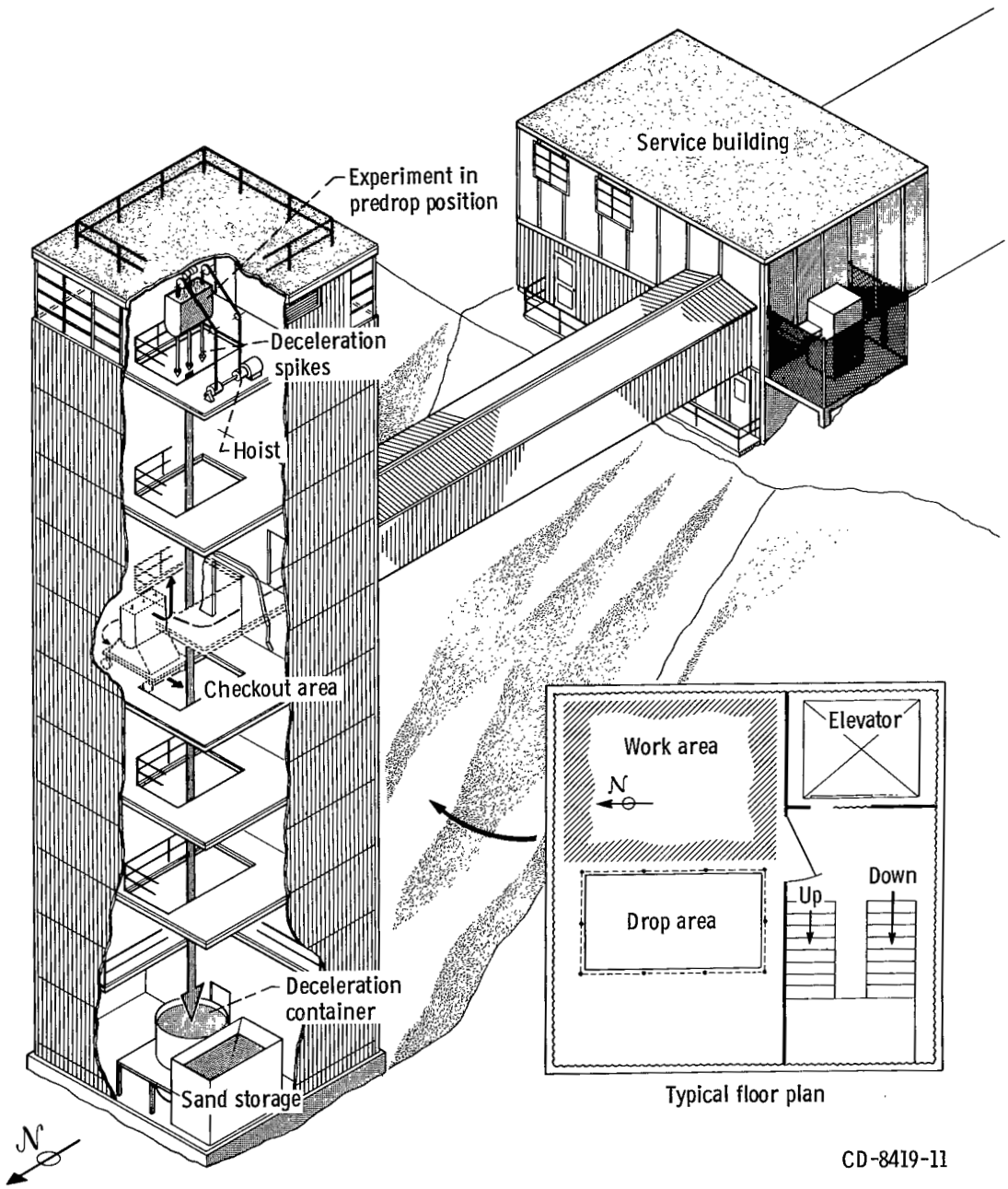

Figure 13. - 2.2-Second Zero-Gravity Facility.

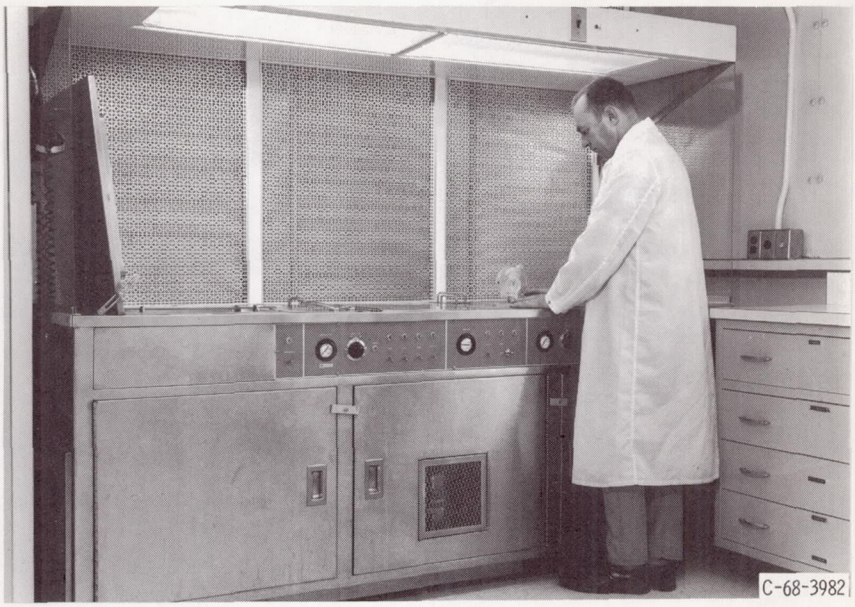

(a) Ultrasonic cleaning system.

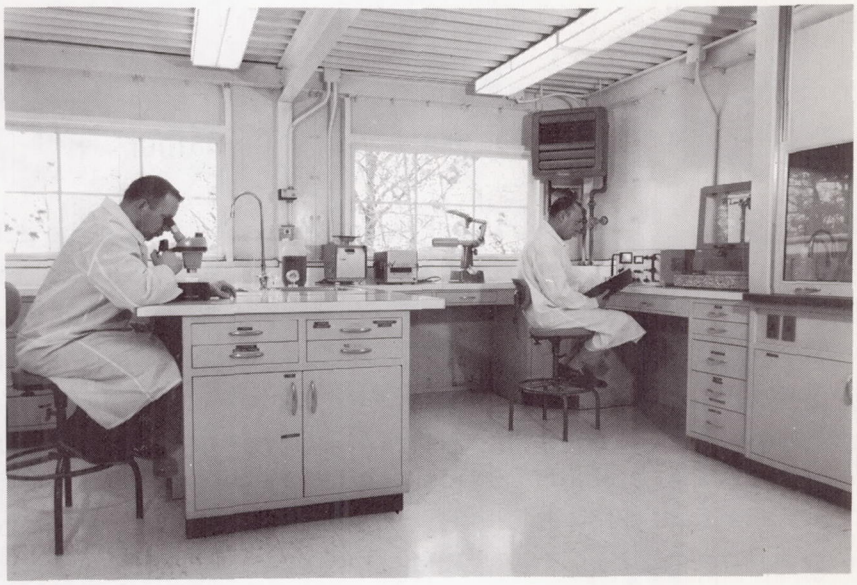

C-68-3983

(b) Laboratory equipment.

Figure 14. - Controlled environment room.

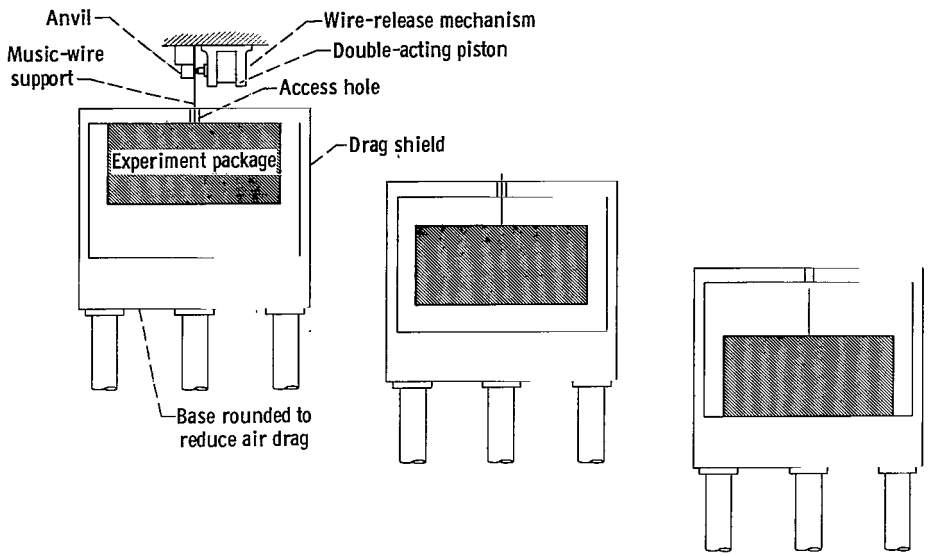

Figure 15. - Position of experiment package and drag shield before, during, and after test drop.

decelerator container, the experiment package has traversed the vertical distance within the drag shield (compare figs. 15(a) and (c)).

Experiment Package and Test Containers

Experiment package. - The experiment package used to obtain the data for this experimental study is shown in figure 16. It consisted of an aluminum frame in which were mounted the experiment tank and pumping system, a 16-millimeter high-speed motion picture camera, a background lighting scheme, and auxiliary equipment. The auxiliary equipment included batteries, a sequence timer, and a digital clock with divisions of 0.01 second. The pumping system is shown in schematic form in figure 17.

Test containers. - Two cylindrical tanks, 2 and 4 centimeters in radius, were used. The tanks, as shown in figure 18, consisted of plastic cylindrical sections, an inlet plate, and selected outlet plates. The cylinders were machined from cast acrylic rod and polished until clear. The length to diameter ratio for the tanks ranged from 4 to 1.5 to allow for testing at various initial liquid heights. In using these tanks, strict geometric similarity was not maintained when the smaller tanks were compared to the larger ones at low initial liquid heights. The distance from the liquid-vapor interface to the pressurant inlet baffle was allowed to vary with initial liquid height. It was felt that since

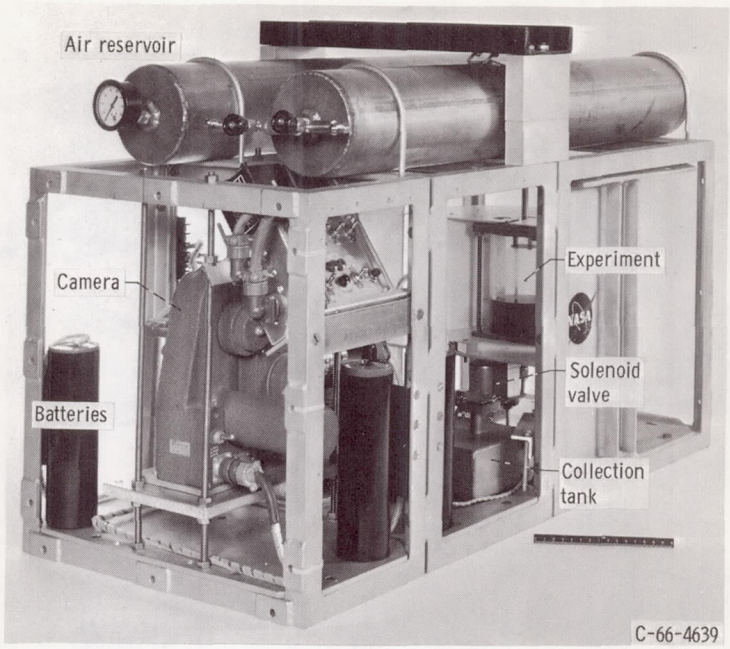

Figure 16. - Vapor ingestion experiment package.

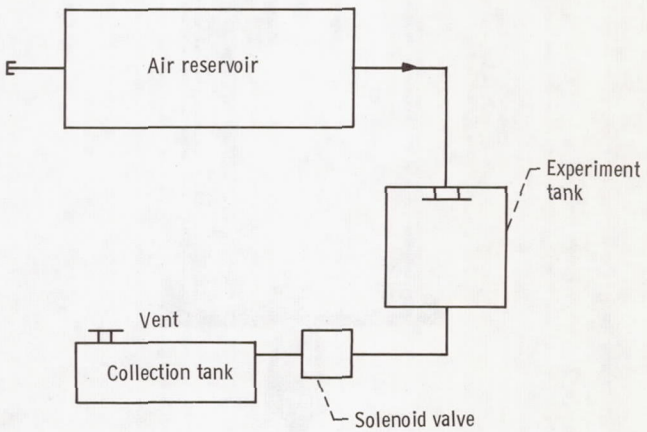

Figure 17. - Pumping system schematic.

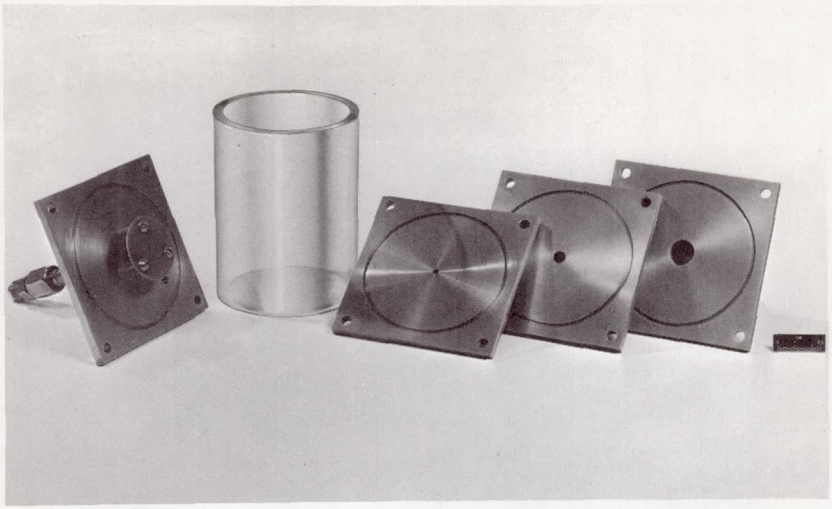

C-67-1210

(a) Typical plastic cylinder, top and bottoms.

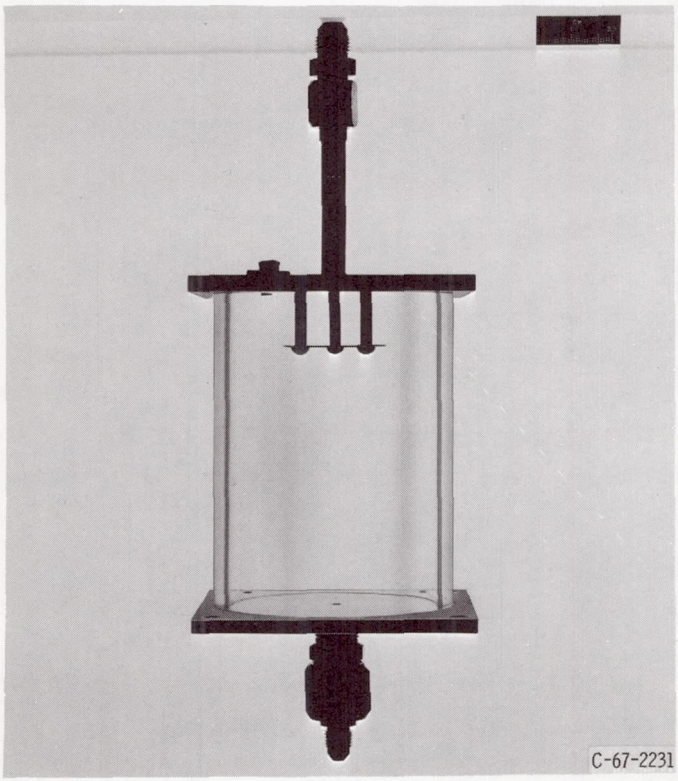

C-67-2231

(b) Assembled tank, including plastic cylinder, top, and bottom.

Figure 18. - Experiment test tanks.

the vapor ingestion phenomenon under investigation was occurring very near to the outlet side of the tanks, the scaling of the vapor space above the liquid had no effect on the results. End plates of stainless steel incorporated "O" ring seals. The inlet of each tank was baffled with a stainless-steel disk, 1 tank radius in diameter, positioned 1/2 tank radius from the face of the inlet (fig. 18). The tank outlets were 0.1, 0.2, and 0.4 centimeter in radius, and each had an outlet length at least 10 times its radius.

Test Procedure

Experiment preparation. - Prior to a test run, the experiment tank parts were cleaned ultrasonically in warm distilled water and detergent, rinsed in distilled water, and dried in a warm-air dryer. The parts were then assembled and installed in the experiment package. The tank was filled with liquid to the desired level and checked for leakage. Draining was accomplished by means of a pressurization technique, using the air reservoir shown schematically in figure 17. This reservoir was charged to a certain pressure. The tank was drained of liquid during both normal-gravity and weightless tests by opening the solenoid valve located downstream of the tank outlet. The volume of air in the reservoir was sufficiently large in comparison with the volume of displaced liquid in the experiment tank that the change in pressure in the experiment tank was negligible during testing.

During normal-gravity testing, draining was initiated at the beginning of the test, and the motion of the liquid-vapor interface was recorded with the high-speed camera. From the resulting film sequence, the interface height as a function of draining time was obtained. For each weightless test, on the other hand, the experiment package was allowed to free fall initially. Sufficient time was allowed for the zero-gravity interface to form. Since the time required for the interface to come to static equilibrium was too long to permit a draining test to follow, initiation of outflow was timed when the interface centerline reached its low point in its first pass through equilibrium. The interface centerline velocity at this time is zero. Draining was then initiated as for normal gravity. The assumption was made that, for a particular calibrated pressure setting in the air reservoir, the resulting outflow rate in the drain was the same in weightlessness as for the normal-gravity test.

Procedure for test drop. - Electrical timers on the experiment package are set to control the initiation and duration of all functions programmed during the drop. The experiment package is then balanced and positioned within the prebalanced drag shield. The wire support is attached to the experiment package through an access hole in the shield (see fig. 15(a)). Properly sized spike tips are installed on the drag shield. Then the drag shield, with the experiment package inside, is hoisted to the predrop position at the top of the facility (fig. 13) and connected to an external electrical power source.

The wire support is attached to the release system and the entire assembly is suspended from the wire. After final electrical checks and switching to internal power, the system is released. After completion of the test, the experiment package and drag shield are returned to the preparation area.

REFERENCES

1. Nussle, Ralph C.; Derdul, Joseph D.; and Petrash, Donald A.: Photographic Study of Propellant Outflow from a Cylindrical Tank During Weightlessness. NASA TN D-2572, 1965.

2. Derdul, Joseph D.; Grubb, Lynn S.; and Petrash, Donald A.: Experimental Investigation of Liquid Outflow from Cylindrical Tanks During Weightlessness. NASA TN D-3746, 1966.

3. Grubb, Lynn S.; and Petrash, Donald A.: Experimental Investigation of Interfacial Behavior Following Termination of Outflow in Weightlessness. NASA TN D-3897, 1967.

4. Gluck, D. F.; Gille, J. P.; Simkin, D. J.; and Zukoski, E. E.: Distortion of the Liquid Surface During Tank Discharge Under Low-G Conditions. Chem. Eng. Progr. Symp. Ser., vol. 62, no. 61, 1966, pp. 150-157.

5. Lubin, Barry T.; and Hurwitz, Matthew: Vapor Pull-Through at a Tank Drain with and without Dielectrophoretic Baffling. Proceedings of the Conference on Long-Term Cryo-Propellant Storage in Space, NASA Marshall Space Flight Center, Huntsville, Ala., Oct. 1966, pp. 173-180.

6. Anon.: Orbital Refueling and Checkout Study. Vol. 3: Evaluation of Fluid Transfer Modes, Part 2. Rep. TI-51-67-21, vol. 3, Lockheed Missiles and Space Co. (NASA CR-93237), Feb. 12, 1968.

NATIONAL AERONAUTICS AND SPACE ADMINISTRATION
WASHINGTON, D. C. 20546

OFFICIAL BUSINESS

FIRST CLASS MAIL

POSTAGE AND FEES PAID
NATIONAL AERONAUTICS AND
SPACE ADMINISTRATION

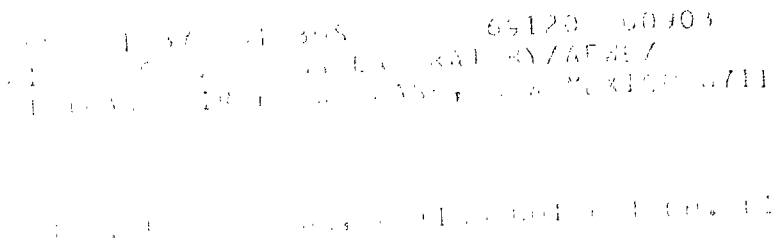

POSTMASTER: If Undeliverable (Section 158 Postal Manual) Do Not Return

"The aeronautical and space activities of the United States shall be conducted so as to contribute . . . to the expansion of human knowledge of phenomena in the atmosphere and space. The Administration shall provide for the widest practicable and appropriate dissemination of information concerning its activities and the results thereof."

—NATIONAL AERONAUTICS AND SPACE ACT OF 1958

NASA SCIENTIFIC AND TECHNICAL PUBLICATIONS

TECHNICAL REPORTS: Scientific and technical information considered important, complete, and a lasting contribution to existing knowledge.

TECHNICAL NOTES: Information less broad in scope but nevertheless of importance as a contribution to existing knowledge.

TECHNICAL MEMORANDUMS: Information receiving limited distribution because of preliminary data, security classification, or other reasons.

CONTRACTOR REPORTS: Scientific and technical information generated under a NASA contract or grant and considered an important contribution to existing knowledge.

TECHNICAL TRANSLATIONS: Information published in a foreign language considered to merit NASA distribution in English.

SPECIAL PUBLICATIONS: Information derived from or of value to NASA activities. Publications include conference proceedings, monographs, data compilations, handbooks, sourcebooks, and special bibliographies.

TECHNOLOGY UTILIZATION PUBLICATIONS: Information on technology used by NASA that may be of particular interest in commercial and other non-aerospace applications. Publications include Tech Briefs, Technology Utilization Reports and Notes, and Technology Surveys.

Details on the availability of these publications may be obtained from:

SCIENTIFIC AND TECHNICAL INFORMATION DIVISION

NATIONAL AERONAUTICS AND SPACE ADMINISTRATION

Washington, D.C. 20546